Polymer 50 (2009) 2142–2148

Contents lists available at ScienceDirect

Polymer

journal homepage: www.elsevier.com/locate/polymer

New insights into the relationship between network structure and strain-induced crystallization in un-vulcanized and vulcanized natural rubber by synchrotron X-ray diffraction

Shigeyuki Toki [a,*], Benjamin S. Hsiao [a,*], Sureerut Amnuaypornsri [b], Jitladda Sakdapipanich [b]

[a] Department of Chemistry, Stony Brook University, Stony Brook, NY 11794, USA
[b] Department of Chemistry, Faculty of Science, Mahidol University, Bangkok 10400, Thailand

ARTICLE INFO

Article history:
Received 27 January 2009
Received in revised form
24 February 2009
Accepted 1 March 2009
Available online 11 March 2009

Keywords:
Strain-induced crystallization
Natural rubber
Network structure

ABSTRACT

The relationship between the network structure and strain-induced crystallization in un-vulcanized as well as vulcanized natural rubbers (NR) and synthetic poly-isoprene rubbers (IR) was investigated via synchrotron wide-angle X-ray diffraction (WAXD) technique. It was found that the presence of a naturally occurring network structure formed by natural components in un-vulcanized NR significantly facilitates strain-induced crystallization and enhances modulus and tensile strength. The stress–strain relation in vulcanized NR is due to the combined effect of chemical and naturally occurring networks. The weakness of naturally occurring network against stress and temperature suggests that vulcanized NR has additional relaxation mechanism due to naturally occurring network. The superior mechanical properties in NR compared with IR are mainly due to the existence of naturally occurring network structure.

1. Introduction

Vulcanized natural rubber (NR) has been studied quite extensively because it is generally considered an ideal network material composed of non-Gaussian chains. Its mechanical behavior appears to obey the concept of rubber elasticity [1,2]. Even though the major component of vulcanized NR is cross-linked *cis*-1,4 poly-isoprene, vulcanized synthetic *cis*-1,4 poly-isoprene rubber (IR) can never match the mechanical properties of vulcanized NR. (In this paper, IR is IR-2200 that is synthetic analogue to NR). Vulcanized IR typically exhibits 70–80% of elastic modulus, tensile strength and tearing resistance of vulcanized NR, despite that raw NR contains 6 wt% of natural "impurities". The inferior mechanical property in vulcanized IR has been attributed to the imperfect (98.5%) stereo-regularity of *cis*-1,4 structure in poly-isoprene compared to the perfect (100%) of *cis*-content in NR.

However, the above hypothesis is not correct because in many ways un-vulcanized NR behaves very differently from un-vulcanized IR, especially one considers that the tensile strength of un-vulcanized NR is almost 60 times higher than that of un-vulcanized IR [3]. (This knowledge is well known in the rubber industry, since IR has been used as an additive to NR to facilitate varying processing steps such as mixing and extrusion.) It is also known that un-vulcanized IR behaves as a polymer melt with typical viscoelastic properties at room temperature because it has a low glass transition temperature (T_g) of −65 °C, whereas un-vulcanized NR behaves more like an elastomer with an stress up-turn characteristic while comprising the same T_g.

Raw (un-vulcanized) NR consists of 94 wt% poly-isoprene molecules and 6 wt% natural components, including proteins (2.2 wt%), phospholipids and neutral lipids (3.4 wt%), carbohydrates (0.4 wt%), metal salts and oxides (0.2 wt%) and others (0.1 wt%) [4]. In contrast, synthetic IR consists of 100% poly-isoprene molecules. It is well known that raw NR is composed of both Gel phase (insoluble part in toluene) and Sol phase (soluble part in toluene) [5]. The term "Gel" means a three-dimensional network that is insoluble in solvents. Thus, the Gel phase in NR is not a true Gel since it is soluble to certain solvents and also soluble at high temperatures [3]. Although the amount of Gel depends on the clones of Hevea tree, ages of tree, periods of storage, storage conditions and processing conditions, the commercial raw NR includes 10–30% of Gel in toluene at room temperature. IR also contains the Gel phase that behaves more like a true gel [6]. The Gel phase in IR is composed of insoluble polymer aggregates (about

* Corresponding authors. Tel.: +1 631 632 7793; fax: +1 631 632 6518.
E-mail addresses: stoki@notes.cc.sunysb.edu (S. Toki), bhsiao@notes.cc.sunysb.edu (B.S. Hsiao).

0032-3861/$ – see front matter © 2009 Elsevier Ltd. All rights reserved.
doi:10.1016/j.polymer.2009.03.001

350 nm in domain size) that are by-products of synthetic polymerization. The increase in Gel content increases the viscosity and modulus of IR. [6]. The commercial IR contains around 10% of Gel.

The stress relaxation behavior in un-vulcanized NR shows much higher modulus and much slower decrease with time than that in un-vulcanized IR [7–9]. In addition, the Gel phase in NR exhibits higher modulus and slower decrease and the Sol phase exhibits lower modulus and faster decrease at longer time than those in original NR [8,9].

Recently, it has been proposed that NR is composed of linear poly-isoprene with two terminal groups [3]. The typical molecular weight of the linear segment between the terminal groups is around 3×10^5 g/mol. This value is not as large as that previously considered, and it is not much different from that of typical IR [3,6,8]. In NR, both terminal groups are active and they can react with natural impurities such as proteins and phospholipids [3]. These reactions can lead to extensions of two linear poly-isoprene segments, connections of three or more linear segments (so-called branches or star), forming a network of different chain connections. As a result, raw NR has been considered as a mixture of connected linear poly-isoprene segments with different connectivity in Fig. 1. This connected mixture is named as the "naturally occurring network" [3]. Therefore, the Gel phase in NR is composed of the naturally occurring connected network, and the Sol phase is composed of extensions and branches of linear chains [3]. The naturally occurring network is thought to be responsible for the elastomeric behavior of un-vulcanized NR.

The strain-induced crystallization in raw (un-vulcanized) NR has been studied extensively [10–17]. For example, the behaviors of strain-induced crystallization in Gel and Sol were first compared in 1937 [13]. Recently, strain-induced crystallization in raw NR, the orientation of strain-induced crystals in raw NR at a deformed state and the comparison of raw NR and de-proteinized (protein is removed) NR (DPNR) have also been reported [14–17]. The results from these studies confirmed the existence of naturally occurring network structure, which is the crucial element responsible for the sharp increase in molecular orientation and the subsequent strain-induced crystallization.

Simultaneous strain-induced crystallization and stress–strain relation in vulcanized NR and IR have been studied by conventional X-ray [18] and by synchrotron X-ray [19–29]. Comparisons of strain-induced crystallization in peroxide and sulfur vulcanized NR and IR have been made [23,30]. Peroxide vulcanized NR showed higher stress and higher crystal fraction than sulfur vulcanized NR did [23]. The onset of crystallization depends on the network density in peroxide vulcanized NR but independent in sulfur vulcanized NR [30]. Peroxide vulcanization does not involve many complex ingredients such as zinc oxide, sulfur and accelerators that sulfur vulcanization requires. Furthermore, the network formed by peroxide vulcanization is simpler than the network formed by sulfur vulcanization since the sulfur bridges between poly-isoprene can be composed of mono sulfur (–*s*–), di-sulfur (–*s*–*s*–) and poly-sulfur (–*s*–s_x–*s*–) linkages.

The objective of the present work is to understand the effects of naturally occurring network and chemical network (through vulcanization) on the mechanical properties in NR using synchrotron X-ray wide-angle X-ray diffraction (WAXD). The chosen base samples (before vulcanization) included purified fresh latex NR preserved in ammonia solution and synthetic IR compounds. Several samples under different preparation were compared, which included chemically treated un-vulcanized NR, the toluene-insoluble fraction of NR (Gel), the toluene-soluble fraction of NR (Sol) and IR. The vulcanization process involved only the peroxide crosslinking reaction. The chemically treated un-vulcanized NR and peroxide vulcanized NR samples provide us a unique opportunity to understand the role of naturally occurring network in the superior mechanical behavior of NR.

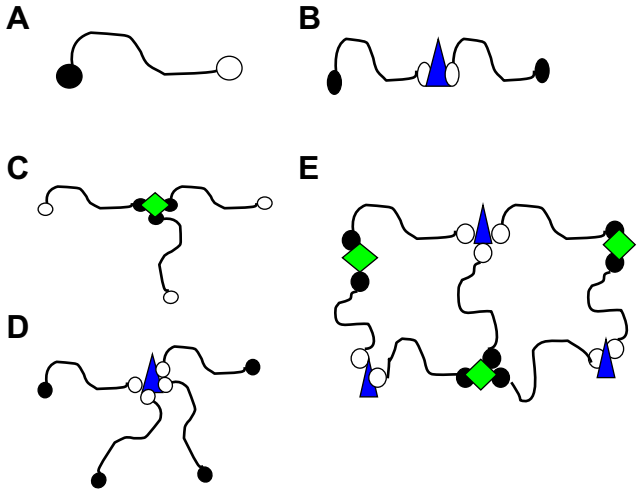

Fig. 1. Schematic models of naturally occurring network. ○: Initiating terminal (ω), ●: terminating terminal (α), ▲ ◆ :natural impurities, A: linear rubber chain unit, B: extension of rubber chains, C: branch of rubber chains, D: star of rubber chains, E: network of rubber chains.

2. Experimental

2.1. Samples and preparation

Raw NR sample used in this study was fresh field latex provided by the Thai Rubber Latex Co, Thailand. The fresh NR latex was preserved with 0.6 v/v% NH_3 (NR latex 100 ml: NH_3 solution 0.6 ml) at room temperature for 3 months. The preserved NR latex was cast on glass dishes and dried in an oven at 50 °C for 24 h. The solid NR was then dissolved in toluene at a concentration of 1 w/v% for one week. Further sample preparation procedures were also applied as follows:

(1) Protein removed. De-proteinized NR (DPNR) was prepared by incubation of the preserved NR latex with 0.04 w/v% proteolytic enzyme (KAO KP-3939) and 1 w/v% Triton®X-100 for 12 h at 37 °C, followed by centrifugation (13,000 rpm, 30 min twice).
(2) Protein and free fatty acid removed. Acetone-extracted DPNR (AEDPNR) was prepared by the extraction of DPNR with acetone at 70 °C for 24 h.
(3) Protein, fatty acids and phospholipids removed by trans-esterification of DPNR (TEDPNR). This process was carried out in toluene solution with freshly prepared sodium methoxide at room temperature for 3 h followed by precipitation with excess amount of methanol. This process removed all naturally occurring network [3].
(4) The separation of Sol and Gel. The toluene solution of NR was separated into heavy part and light part by centrifugation (10,000 rpm, 30 min). The lighter part was the Sol phase that was composed of toluene-soluble rubber fractions and soluble natural components. The heavier part was the Gel phase that contained insoluble connected rubber fractions and insoluble natural impurities.
(5) Synthetic *cis*-1,4 poly-isoprene (IR) used in this study was IR-2200 manufactured by JSR.
(6) DPNR+P, i.e., DPNR with the extracted proteins added back to the sample. Proteins were extracted from fresh NR latex by washing with surfactant and precipitating with cold acetone.

The extracted proteins were dissolved in the DPNR latex and kept for one month.

All of the above samples were dissolved in toluene as 3 w/v% solution. These solutions were cast onto glass dishes, after solvent evaporation leading to the as-cast films (about 1 mm thick). The recovered films were characterized by SAXS, WAXD and optical microscopy techniques.

The vulcanization conditions (by peroxide reaction) were as follows. Un-vulcanized rubber samples were first masticated by a two-roll mill at 50 °C for 2 min. Subsequently, 1 phr (per hundred rubber) peroxide (DCP: dicumyl peroxide) was added in these samples and thoroughly mixed for 3 min. The rubber compounds were vulcanized at 155 °C for 30 min in the 1 mm depth mold by compression.

2.2. Sample characterization

Synchrotron X-ray measurements were carried out at the X27C beam line in the National Synchrotron Light Source (NSLS), Brookhaven National Laboratory (BNL). The wavelength of the X-rays used was 1.371 Å. Two-dimensional WAXD patterns were recorded by an MAR-CCD detector (MAR USA). The image acquisition time for each frame was 30 s. The diffraction angle in WAXD was calibrated by the Al_2O_3 standard. All measured images were corrected for beam fluctuations and sample absorption. The data analysis software POLAR (Stonybrook Technology and Applied Research, New York) was used to analyze the WAXD images.

A tensile stretching device, allowing the symmetric deformation of the sample, was used in this study. The device permitted the illumination of X-ray to monitor the structure change on the same sample position during deformation. This instrument was developed by modifying a tabletop stretching machine from the Instron Inc. The chosen deformation rate was 10 mm/min. The original sample length was 25 mm. The initial rate of deformation was 0.007 s^{-1}. The nominal stress was given by $\sigma = F/(d_0 \times w_0)$, with F being the force measured by a load cell, d_0 being the original thickness and w_0 being the original width. The nominal strain, in terms of the deformation ratio, was given by $\varepsilon = (l - l_0)/l_0$ with l_0 being the original clamp-clamp distance.

The stress–strain relation measurements during extension and retraction in uniaxial deformation were carried out at 25 °C. In the case of stress relaxation, and temperature variation experiments, the stretching processes were carried out at 30 °C for the former and the rate of increasing temperature were +2 °C/min., respectively. These studies were carried out in an environmental chamber. Time-resolved WAXD patterns and simultaneous stress–strain curve were recorded continuously during stretching, retraction, stress relaxation at 30 °C, and upon heating.

3. Results and discussion

3.1. Un-vulcanized NR and un-vulcanized IR

The latex sample preserved in ammonia for three months was chosen because this specimen possessed almost the same amount of Gel content and the same level of tensile strength as the commercial raw NR sample (i.e., technically standard rubber, TSR, or ribbed smoked sheet, RSS)[3]. The preservation of fresh latex in the presence of ammonia creates a naturally occurring network and increases tensile strength and gel content [3]. Such sample selection also avoided potential adverse effects from abrasive processing steps, such as milling, fracturing, drying and smoking that are commonly adopted to manufacture commercial raw NR. The stress–strain curves of raw NR, Gel, Sol, TEDPNR (transesterificated and de-proteinized NR) and raw IR samples at 25 °C are shown in Fig. 2. The Gel sample exhibits a large up-turn and higher stress than NR, the Sol sample shows relatively lower stress, and TEDPNR shows the lowest stress since TEDPNR has no naturally occurring network [3]. IR shows the lower stress than NR samples except TEDPNR. It is found that TEDPNR and raw IR sample cannot be extended more than the strain of 2.0 because the width of the center part of the sample becomes too narrow to bear the load. The NR, Gel and Sol samples have no such a problem, but they show clear hysteresis with a permanent set at a strain about 1.6. It is interesting to note that that the Sol sample exhibited a distinct elastic rubbery behavior. However, the naturally occurring network seems to be weak against the stress. This is because the permanent sets of NR, Gel and Sol are much larger than the one of vulcanized NR (almost zero).

Un-vulcanized NR, Gel and Sol samples all exhibit the behavior of strain-induced crystallization. Fig. 3 shows the stress–strain relation and strain-induced crystallization of un-vulcanized NR during extension and retraction. Although the diffracted intensity in un-vulcanized NR is relatively low, WAXD patterns clearly show the occurrence of strain-induced crystallization at strains above 4.0. The behavior of strain-induced crystallization in un-vulcanized NR is very similar to vulcanized NR.

In order to measure the small amount of strain-induced crystallinity due to the weak intensity of the WAXD pattern in the deformed sample, only the equator diffraction peaks were analyzed. In specific, the diffraction intensity near the equator from 265° to 275° was integrated and termed as the total intensity ($I(s)_{\text{total}}$), whereas the intensity near the meridian from −5° to +5 was also integrated and termed as the amorphous intensity ($I(s)_{\text{amorphous}}$). It has been assumed that the intensity around the meridian is mainly due to the scattering of un-oriented amorphous molecules. Fig. 4 illustrates the above analytical procedure, where the chosen WAXD pattern was from the deformed un-vulcanized NR sample at a strain of 6.0. In Fig. 4, the image indicated an oriented fiber pattern consisting of arc-like crystal diffraction peaks from the polymer as well as spot-like diffraction peaks of very high intensity (these diffraction spots are related to the discrete nanocrystals of natural impurities in NR, where details were reported elsewhere [31]).

The equatorial integration from 265° to 275° allowed us to avoid the contribution of these high intensity spots in the analysis of integrated intensity. The crystalline intensity ($I(s)_{\text{crystal}}$) can be given as:

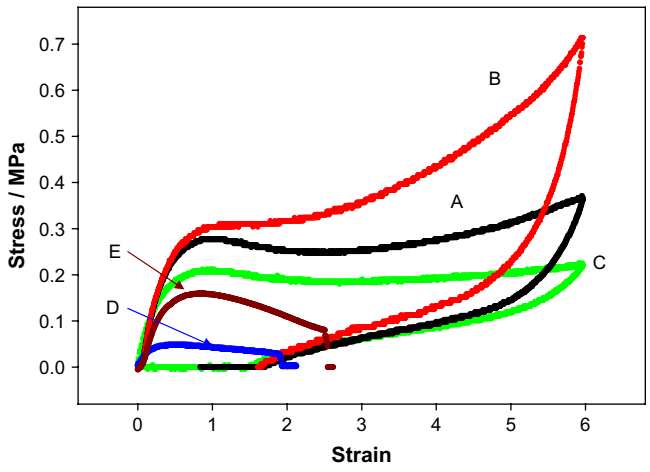

Fig. 2. Stress–strain relations during extension of un-vulcanized poly-isoprene at 25 °C, A: NR, B: Gel, C: Sol, D: TEDPNR, E: IR.

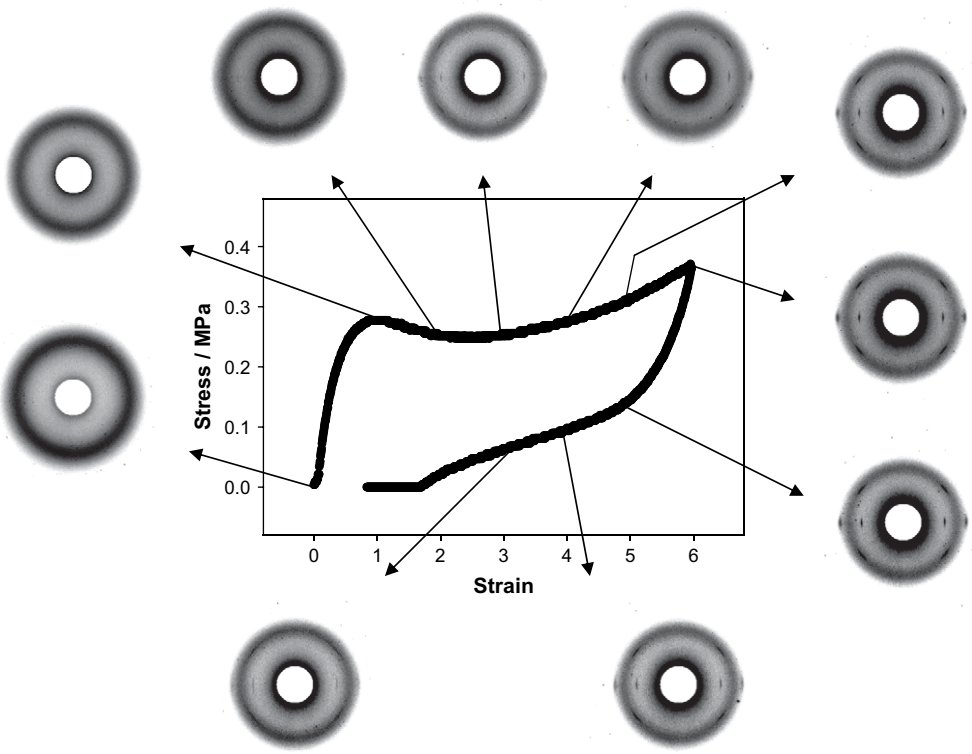

Fig. 3. Stress–strain relation and selected WAXD patterns during extension and retraction of un-vulcanized NR at 25 °C. Each image was taken at the average strain indicated by the arrow.

$$I(s)_{\text{crystal}} = I(s)_{\text{total}} - I(s)_{\text{amorphous}} \quad (1)$$

The subtracted crystalline intensities of un-vulcanized NR at different strain are shown in Fig. 5. It is found that the diffraction intensities at 200 and 120 planes increase with strain significantly.

The intensity at the 200 plane ($s = 1.58\ \text{nm}^{-1}$) was chosen to estimate the change of the crystallinity index, which was defined as the ratio of the crystalline intensity from (200) reflection and the total intensity at $s_c = 1.58\ \text{nm}^{-1}$.

$$\text{Crystallinity Index}\,(200) = I(s_c)_{\text{crystal}}/I(s_c)_{\text{total}} \times 100 \quad (2)$$

Fig. 6 shows the Crystallinity Index (200) in NR, Gel, Sol, TEDPNR and IR at different strains during extension. NR and Gel samples exhibit clear behavior of strain-induced crystallization. TENR and IR samples do not show any strain-induced crystallization. The Sol sample only shows a small amount of strain-induced crystallization at higher strains. The results confirm that the naturally occurring network is mainly responsible for the behavior of strain-induced crystallization in un-vulcanized NR. The observation in the Sol sample is probably indicative that Sol has a smaller amount of network points than NR and Gel samples.

The above finding is rather surprising because the Sol phase is often considered to contain mainly low molecular weight species. However, this hypothesis may not be correct. Recently, Tanaka has carefully compared the molecular weight distribution of the Sol

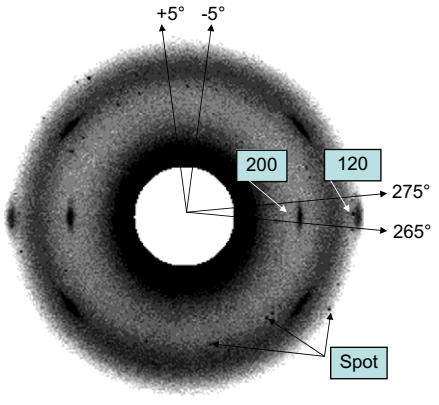

Fig. 4. The WAXD pattern of un-vulcanized NR at strain 6.0. The arrows 265° and 275° suggest the integral angle for $I(s)_{\text{total}}$ and the arrows −5 and +5 suggest the integral angle for $I(s)_{\text{amorphous}}$. High intensity spots are shown by arrows.

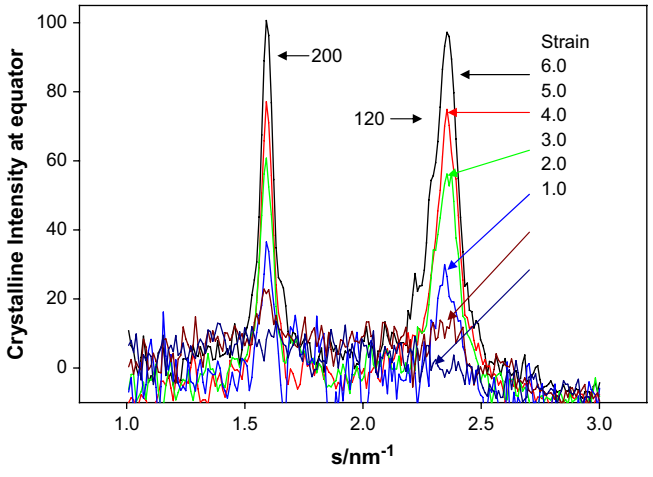

Fig. 5. Crystalline intensities at equator in un-vulcanized NR at different strains.

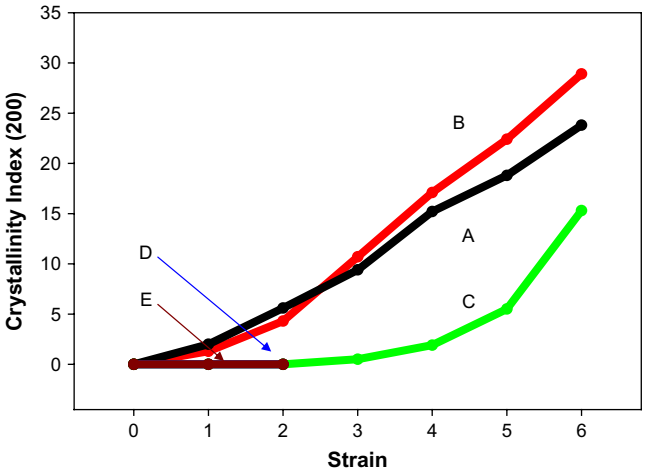

Fig. 6. Crystallinity index for the (200) reflection of un-vulcanized samples. A: NR, B: Gel, C: Sol, D: TEDPNR, E: IR.

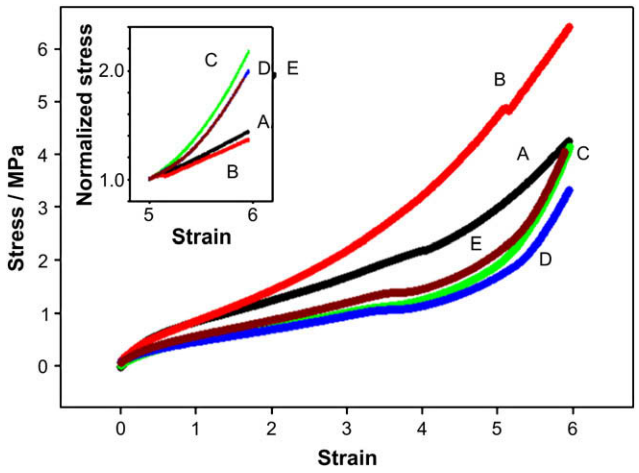

Fig. 7. Stress–strain relations of A: V-NR, B: V-Gel, C: V-Sol, D: V-TEDPNR, E: V-IR at 25 °C.

fraction and the transesterified Gel fraction (TE-Gel) in un-vulcanized NR [3]. He reported that the weight average molecular weight (M_w) of the Sol fraction was 2.52×10^6 g/mol in one large population, whereas the M_w of TE-Gel was 1.25×10^6 g/mol in two populations. Therefore, the Sol fraction in un-vulcanized NR does not necessarily consist of only the low molecular species, it may also contain extensions, branches, permanent entanglements, or/and a low density network of linear molecular species with both terminal functional groups capable of reacting with proteins and phospholipids as those in the Gel sample. In Fig. 2, the stress–strain curve in the Sol sample exhibits the appearance of a yield point and constant stress after yielding (i.e., the plastic flow behavior). This behavior is similar to that of an entangled polymer melt. Since the entanglement molecular weight (M_e) in *cis*-1,4 poly-isoprene is about 3000 g/mol at 25 °C [32], each chain may statistically contain around 100 entanglement points and the overall entanglement structure may contribute to the mechanical behavior of un-vulcanized NR. Based on the WAXD results, one may conclude that the behavior of strain-induced crystallization in the Sol sample is not induced by stress but by strain, since the corresponding stress at the onset of crystallization is very low. This is the main reason that we have persistently used the term "strain-induced crystallization" instead of "stress-induced crystallization" to describe the phenomenon.

3.2. Peroxide vulcanized NR and IR

Stress–strain relations in peroxide vulcanized NR (V-NR), vulcanized Gel (V-Gel), vulcanized Sol (V-Sol), vulcanized TEDPNR (V-TEDPNR) and vulcanized IR (V-IR) are shown in Fig. 7. The different stress–strain relations can be attributed to the different amount of the naturally occurring network since the chemical network density should be the same in these samples due to the same amount of peroxide used. V-Gel and V-NR samples show much higher values of stress at small strains than V-Sol, V-TEDPNR and V-IR samples. At large strains, the stress levels of V-Sol, V-TEDPNR and V-IR catch up those of V-NR and V-Gel. Since V-Sol, V-TEDPNR and V-IR increase their stresses steeply around the strain of 6.0, these samples all exhibit the same strain at break (6.0). The inset figure in Fig. 7 shows the steep increase of the stresses of these samples from the strain 5.0–6.0 as normalized stress. (Normalized stress = stress/stress at strain 5.0). V-Sol, V-TEDPNR and V-IR increase much larger than V-NR and V-Gel.

According to the theory of rubber elasticity, the strain at break depends on the molecular weight between the network points due to the limited extensibility [1,2,34,35]. Both non-Gaussian chain models [1,2,33] and non-Gaussian tube models [34,35] elucidate that the steep increase of stress is induced close to the strain at break. The steep increase of stress has been expressed as the divergence of inverse Langevin equations in the non-Gaussian chain model and as the singularity in the non-Gaussian tube model. The molecular weight between the network points (M_c) is proportional to the inverse of the number (N_c) of chains per unit volume that is determined by the amount of peroxide used.

$$M_c = \rho N_a / N_c \tag{3}$$

In the above equation, ρ is the polymer density and N_a is Avogadro's constant. Since the number of the chemical network in V-IR and in V-TEDPNR is the same, a similar strain at break value should be observed. On the other hand, V-NR and V-Gel should exhibit prominent mechanical enhancement (i.e., large strain at break values) due to the presence of naturally occurring network. These behaviors have all been confirmed experimentally (Fig. 7). The amount of the naturally occurring network in V-Sol seems to be too low to effectively enhance the stress–strain curve. In the above consideration, the effect of entanglements on the mechanical properties has been neglected in spite of that many entanglements must be permanently imprinted into the structure after vulcanization (this is because the entanglement molecular weight M_e (3000 g/mol) is much lower than the M_n value (3×10^5 g/mol) of the linear unit chain of NR).

The behavior of steep stress increase in V-Sol, V-TEDPNR and V-IR indicates that these vulcanized NR samples probably reach the limit of chain extensibility between the network points at such high strains. The presence of naturally occurring network in V-Gel and V-NR seems to increase the limit of chain extensibility. This may be because the naturally occurring network can relax the effective stress on the final network structure as the much weaker naturally occurring network (compared to the chemical network) can be destroyed at high strains. The maximum value of strain at break $\varepsilon_{b,max}$ has been routinely used as an effective way to determine the failure envelop in rubber [36,37]. The failure envelope is well correlated with the degree of crosslinking. Based on the theory of rubber elasticity, the maximum value of strain at break $\varepsilon_{b,max}$ can be correlated with the molecular weight between two adjacent cross-links (M_c) [36]:

$$\varepsilon_{b,max} + 1 \propto M_c^{1/2} \quad (4)$$

In Fig. 7, V-Sol, V-TEDPNR and V-IR show the same value of strain at break that can be attributed to the same amount of the chemical network in the samples. On the other hand, V-NR and V-Gel show larger values of stress than those in V-Sol, V-TEDPNR and V-IR. Although the presence of the naturally occurring network should lead to a slight decrease in strain at break, both V-NR and V-Gel samples indicate that they have the same value of (or slightly larger) strain at break as the other samples (V-Sol, V-TEDPNR and V-IR).

Peroxide vulcanized NR show smaller value of strain at break or higher value of stress at affixed strain than those of sulfur vulcanized NR. This is because peroxide vulcanization does not have the same stress relaxation mechanism as sulfur vulcanization, where the transformations of sulfur bridges from multi-sulfur to mono or di-sulfur bridges often occur [39]. The naturally occurring network in V-NR and V-Gel seem to relax the stress and extend the value of strain at break as the naturally occurring network is significantly weaker than chemical network.

The crystallinity index based on the (200) reflection of the vulcanized samples is shown in Fig. 8. It is seen that the values of V-NR, V-Gel and V-Sol are twice of that of un-vulcanized NR in Fig. 6. The presence of chemical network increases the behavior of strain-induced crystallization significantly. Although un-vulcanized TEDPNR and IR sample did not exhibit the sign of strain-induced crystallization in Fig. 6, vulcanized samples (V-TEDPNR, V-IR) show higher crystallization than those of V-NR and V-Gel in Fig. 8. This indicates that the naturally occurring network in un-vulcanized NR and Gel does not increase the strain-induced crystallization in V-NR and V-Gel necessarily. V-Sol, V-TEDPNR and V-IR samples show almost the same level of crystalline fraction and the maximum value at strain 5.0. Therefore, the strain-induced crystallization in vulcanized NR appears to saturate at a critical strain that is significantly less than the strain at break. The saturation of strain-induced crystallization in vulcanized NR has been observed in the literature before [23,38], although this behavior has never been discussed. The divergence behaviors of the sharp stress up-turn and the saturation of strain-induced crystallization at large strains constitute two essential mechanisms in strain-induced crystallization. This can be further explained as follows. During extension, both molecules and network points shifted to a more stable state to accommodate the stress. As a result, orientation and crystallization of chains take place simultaneously. This mechanism would reduce the stress as

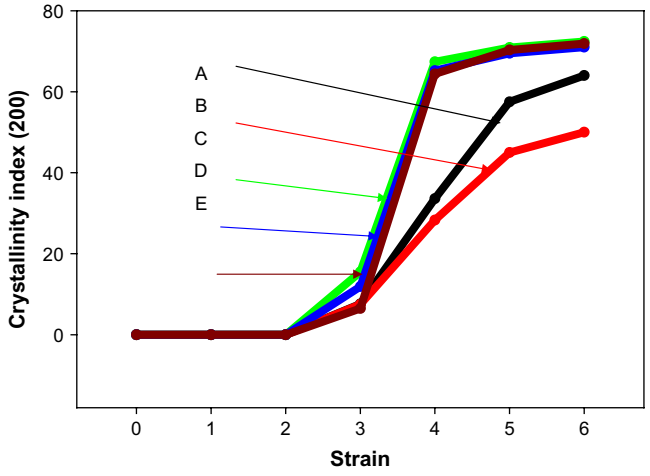

Fig. 8. Crystallinity index for the (200) reflection of A: V–NR, B: V-GR, C: V:Sol, D: TEDPNR, E: V-IR.

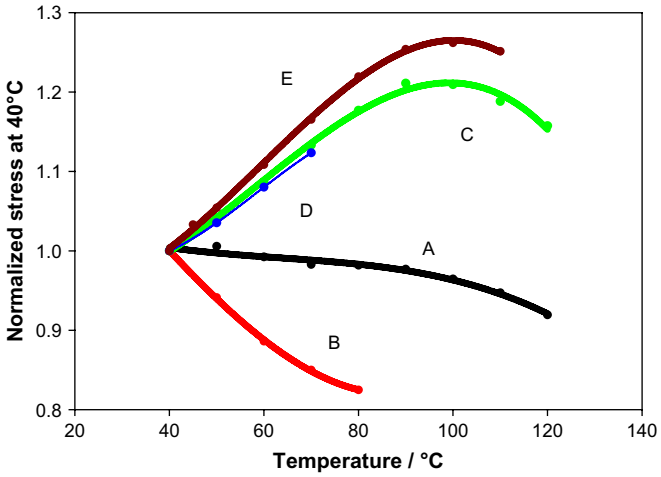

Fig. 9. Normalized stresses at restrained heating in peroxide vulcanized samples. A: V-NR, B: V-Gel, C: V-Sol, D: V-TEDPNR, E: V-IR.

discussed earlier [18,29,40–42] on theoretical analysis by Flory [40] and experimentally by Gent [41] because the length of crystallized chains along the stretching direction is longer than the one of oriented amorphous chains. However, beyond a certain strain, molecules cannot find room to crystallize, the degree of strain-induced crystallization reached the certain limit. At higher strain, the remained amorphous molecules look for room to orient itself, finally amorphous molecules reach the limit of extensibility. At such a strain level (near the limit of extensibility), the stress would diverge following the theories of non-Gaussian chain model and tube model. Therefore, strain-induced crystallization does not contribute to increase the tensile strength but increase the strain at break since the strain-induced crystalline molecule is longer than oriented amorphous chain along the stretched direction. This mechanism has been discussed in vulcanized IR [42] and in filled vulcanized NR [43]. In the case of V-NR and V-IR samples, the maximum strain-induced crystallinity seems to be around 30% [19,21,22,24,41]. It thus suggests that the poly-isoprene molecules cannot crystallize beyond a certain level of crystallization since both network points and chain entanglements are obstacles to the occurrence of strain-induced crystallization at higher strains. In the case of cold crystallization (under static condition at −25 °C), un-vulcanized NR shows the saturation of crystallization below 40% [44,45].

After stretched to the strain of 4.0 at 30 °C, all samples were subjected to the treatment of constrained heating (at the strain of 4.0) at a rate of 2 °C/min. The normalized stress (=stress at certain temperature/stress at 40 °C) during constrained heating is shown in Fig. 9. It is found that the stress increases with temperature in V-Sol, V-TEDPNR and V-IR samples, whereas the stress decreases significantly in V-NR and V-Gel. This clearly suggests that the naturally occurring network affects the temperature dependency of vulcanized NR. Since the naturally occurring network is relatively weak against solvents [3], temperature and stress, V-NR and V-Gel show the same trend under these conditions. Recently, we have reported the restrained heating of sulfur vulcanized IR at different strains using synchrotron WAXD [29]. It was found that the strain-induced crystal fraction decreases and the stress increases by temperature. This tendency is enhanced in sulfur vulcanized IR. In Fig. 9, peroxide vulcanized IR shows the same behavior as sulfur vulcanized IR [29].

4. Conclusions

The natural impurities and linear rubber chains with functional end groups in NR create naturally occurring network structure that

significantly affects the mechanical properties of both un-vulcanized and vulcanized NR. The superior mechanical performance in NR (as compared to IR) can be summarized as follows.

1. Strain-induced crystallization is introduced by the naturally occurring network in un-vulcanized NR and the combined network structure (chemical and naturally occurring networks) in vulcanized NR. The final network structure is the vital element for strain-induced crystallization as the network points that are able to align the chains under tensile deformation.
2. The maximum strain at break due to the maximum extensibility of chains between the network points is determined by combined effects of the network structure and strain-induced crystallization. Generally, strain-induced crystallization decreases the stress and increases the strain at break. But the degree of strain-induced crystallization saturates below the strain at break as the molecules may have no room to move to the minimum energy position at high strains.
3. The naturally occurring network decreases the stress at high temperatures since such a network is relatively weak against temperature and stress. This may be one of the reasons why the stress and tensile strength in vulcanized NR decrease with temperature. In addition, the naturally occurring network contributes to the increase in stress at small and medium strains. At large strains, the naturally occurring network relax the stress concentration and increase the strain at break. The above mechanisms may elucidate why the mechanical performance of NR is superior to IR.

Acknowledgement

The financial support of this study was provided by the National Science Foundation (DMR-0405432) with a special two-year Creativity Award extension, Yokohama Rubber, Sumitomo rubber, Bridgestone and a grant from the Thailand Research Fund PHD/0142/2546, the Commission on Higher Education RMU4980046.

References

[1] Treloar LRG. The physics of rubber elasticity. 3rd ed. Oxford University Press; 1975.
[2] Boyce C, Arruda EM. Constitutive models of rubber elasticity; a review. Rubber Chem Technol 2000;73:504.
[3] Tanaka Y. Structural characterization of natural polyisoprene based on structural study. Rubber Chem Technol 2001;74:355.
[4] Alk-Hwee Eng, Tanaka Y. Structure of natural rubber. Trends Polym Sci 1993;3:297.
[5] Allen PW, Bristow GM. The gel phase in natural rubber. J Appl Polym Sci 1963;7:603–15.
[6] Grechnovskii VG, Poddurenyi IYa, Ivanova LS. Molecular structure and macroscopic properties of synthetic cis-poly(isoprene). Rubber Chem Technol 1974;47:342.
[7] Montes S, White JL. A comparative rheological investigation of natural and synthetic cis-1,4 polyisoprenes and their carbon black compounds. Rubber Chem Technol 1982;55:1354.
[8] Campbell DS, Fuller KNG. Factors influencing the mechanical behavior of raw unfilled natural rubber. Rubber Chem Technol 1984;57:104.
[9] Fuller KNG. Rheology of raw rubber. In: Roberts AD, editor. Natural rubber science and technology. Oxford University Press; 1988 [chapter 5].
[10] Katz JR. X-ray scattering investigation of stretched rubber and its possible significance for the problem of the stretching properties of the material. Die Naturwissenschafen 1925;19:410.
[11] Katz JR. What are the reasons for the characteristic elasticity of rubber? II. The joule effect and the new structure of the substance arranged in three dimensions by the stretching. Kolloid Z 1925;37(1):19–22.
[12] Katz JR. What are the reasons for the characteristic elasticity of rubber? 1. The changing of the X-ray spectrum of rubber on stretching. Kolloid Z 1925;36(5):300–7.
[13] Clark GL, Wolthuis E, Smith WH. X-ray diffraction patterns of sol, gel and total rubber when stretched, and when crystallized by freezing and from solutions. J Research National Bureau Stand 1937;19(4):479–91.
[14] Rahman N, Isanasari A, Anggraeni R, Honggokusumo S, Iguchi M, Masuko T, et al. Modern interpretation on the high-stretching of natural rubber attained by the classic 'racking' method. Polymer 2003;44:283.
[15] Alam MM, Asano T. Biaxial orientation mechanism of drawn natural rubber. I. Appearance of the biaxial orientation. J Macromol Sci Part B Phys 2006;45:753.
[16] Toki S, Sics I, Hsiao B, S Amnuaypornsri S, Kawahara S. Strain-induced crystallization in un-vulcanized natural rubbers by synchrotron X-ray study. Rubber Division ACS Fall meeting; 2005, Paper #75.
[17] Amnuaypornsri S, Toki S, Hsiao BS, Sakdapipanich J, Tanaka Y. Strain-induced crystallization of natural rubber: effect of proteins and phospholipids. Rubber Chem Technol 2008;81:753.
[18] Toki S, Fujimaki T, Okuyama M. Strain-induced crystallization of natural rubber as detected real time by wide angle X-ray diffraction technique. Polymer 2000;41:5423.
[19] Lee DJ, Donovan JA. Microstructural changes in the crack tip region of filled natural rubber. Rubber Chem Technol 1987;60:910.
[20] Murakami S, Senoo K, Toki S, Kohjiya S. Structural development of natural rubber during uniaxial stretching by in situ wide angle X-ray diffraction using a synchrotron radiation. Polymer 2002;43:2117.
[21] Toki S, Sics I, Ran S, Liu L, Hsiao BS, Murakami S, Senoo K, et al. New insights into structural development in natural rubber during uniaxial deformation by in situ synchrotron X-ray diffraction. Macromolecules 2002;35:6578.
[22] Trabelsi S, Alobouy PA, Rault J. Stress-induced crystallization around a crack tip in natural rubber. Macromolecules 2002;35:10054.
[23] Toki S, Sics I, Ran S, Liu L, Hsiao BS. Molecular orientation and structural development in vulcanized polyisoprene rubbers during uniaxial deformation by in situ X-ray diffraction. Polymer 2003;44:6003.
[24] Toki S, Sics I, Hsiao BS. Nature of strain-induced structures in natural and synthetic rubbers under stretching. Macromolecules 2003;36:5915.
[25] Trabelsi S, Alobouy PA, Rault J. Crystallization and melting processes in vulcanized stretched natural rubber. Macromolecules 2003;36:7624.
[26] Trabelsi S, Alobouy PA, Rault J. Effective local deformation in stretched filled rubber. Macromolecules 2003;36:9093.
[27] Tosaka M, Murakami S, Poompradub S, Kohjiya S, Ikeda Y, Toki S, et al. Orientation and crystallization of natural rubber network as revealed by WAXD using synchrotron radiation. Macromolecules 2004;37:3299–309.
[28] Toki S, Sics I, Hsiao BS, Murakami S, Tosaka M, Poompradub S, et al. Structural developments in synthetic rubbers during uniaxial deformation by in situ cynchrotron X-ray diffraction. J Polym Sci Part B Polym Phys 2004;42:956–64.
[29] Toki S, Sics I, Hsiao BS, Murakami S, Tosaka M, Poompradub S, et al. Proving the nature of strain-induced crystallization in polyisoprene rubber by combined thermomechanical and in situ X-ray diffraction techniques. Macromolecules 2005;38:7064.
[30] Ikeda Y, Yasuda Y, Hijikata K, Tosaka M, Kohjiya S. Comparative study on strain-induced crystallization behavior of peroxide cross-linked and sulfur cross-linked natural rubber. Macromolecules 2008;41:5876.
[31] Toki S, Burger C, Hsiao BS, Amnuaypornsri S, Sakdapipanich J. Multi-scaled microstructures in natural rubber characterized by synchrotron x-ray scattering and optical microscopy. J Polym Sci Part B Polym Phys 2008;46(22):2456–64.
[32] Fetters LJ, Lohse DJ, Richter D, Witten TA, Zirkel A. Connection between polymer molecular weight, density, chain dimensions, and melt viscoelastic properties. Macromolecules 1994;27(14):4639.
[33] Gent AN. A new constitutive relation for rubber. Rubber Chem Technol 1996;69:59.
[34] Edwards SF, Vilgis TA. The tube model-theory of rubber elasticity. Rep Prog Phys 1988;51:243–97.
[35] Kluppel M, Meng H, Schmidt H, Schneider H, Schuster RH. Influence of preparation conditions on network parameters of sulfur-cured natural rubber. Macromolecules 2001;34:8107–16.
[36] Gent AN. Rubber elasticity: basic concepts and behavior. In: Mark JE, Erman B, Eirich FR, editors. Science and technology of rubber. 2nd ed. Academic press; 1994 [chapter 1].
[37] Smith TL, Chu WH. Ultimate tensile properties of elastomers 7. Effect of crosslink density on time-temperature dependence. J Polym Sci A-2 Polymer Physics 1972;10(1):133.
[38] Tosaka M, Kohjiya S, Murakami S, Poompradub S, Ikeda Y, Toki S, et al. Effect of network chain length on strain-induced crystallization of NR and IR vulcanizates. Rubber Chem Technol 2004;77:711.
[39] Nakauchi H. Characterization of network structure in vulcanized rubber by the compression swell method. J Soc Rubber Ind Japan 2002;75:73.
[40] Flory PJ. Thermodynamics of crystallization in high polymers. 1. Crystallization induced stretching. J Chem Phys 1947;15:397.
[41] Gent AN. Crystallization and the relaxation of stress in stretched natural rubber vulcanizates. Trans Faraday Soc 1954;50:521.
[42] Miyamoto Y, Yamano H, Sekimoto K. Crystallization and melting of polyisoprene rubber under uniaxial deformation. Macromolecules 2003;36:6462–71.
[43] Toki S, Minouchi N, Sics I, Hsiao BS, Kohjiya S. Synchrotron X-ray scattering: tensile strength and strain-induced crystallization in carbon black filled natural rubber. Kautschuk Gummi Knststoffe 2008;61:85.
[44] Kawahara S, Kakubo T, Sakdapipanich JT, Isono Y, Tanaka Y. Characterization of fatty acids linked to natural rubber- role of linked fatty acids on crystallization of the rubber. Polymer 2000;41:7483–8.
[45] Chenal JM, Chazeau L, Bomal Y, Cauthier C. New insights into the cold crystallization of filled natural rubber. J Polym Sci Part B Polym Phys 2007;45:955–62.